Preparation of PVP-BiOBr Adsorbent for Efficient Indigo Carmine Dye Removal Using Flow-Circulation Systems

Saowapak Teerasong,* Thanakrit Saenghirun, Thanawat Sunthornchainukul, Supinya Thammaso, Apiwat Chompoosor, and Suwat Nanan

Read Online

ACCESS | Metrics & More | Article Recommendations | Supporting Information

ABSTRACT: This work presents an adsorptive removal of indigo carmine (IC) dye using a polyvinylpyrrolidone capped bismuth oxybromide (PVP-BiOBr) adsorbent. PVP-BiOBr was synthesized via a simple precipitation method. The morphology and surface chemical structure of the adsorbent were characterized using XRD, SEM, FTIR, and BET analyses. The adsorption isotherm and kinetics were investigated to reveal the mechanism of dye removal. Prepared PVP-BiOBr has a crystallite size of 19.7 nm, with a mean particle size of $\sim 2 \mu m$ and a surface area of $5.14 \ m^2 \ g^{-1}$. The optimum pH for this adsorptive process spanned the range of 4 to 9. Experimental data indicated applicability of the Langmuir isotherm model, and the study confirms a pseudo-second-order kinetics model. The maximum adsorption capacity for IC dye was $208.3 \ mg \ g^{-1}$. A flow-circulation system was developed for the treatment of IC dye contaminated water samples. PVP-BiOBr was packed inside a column and did not spill into the water sample after treatment. The removal efficiency was ≥90% after 25 min. The PVP-BiOBr adsorbent could be reused for three cycles. This work demonstrates that PVP-BiOBr is a promising candidate as an adsorbent for IC dye removal. Additionally, the flow-based system establishes an automated operation in continuous mode, which is viable for large scale applications.
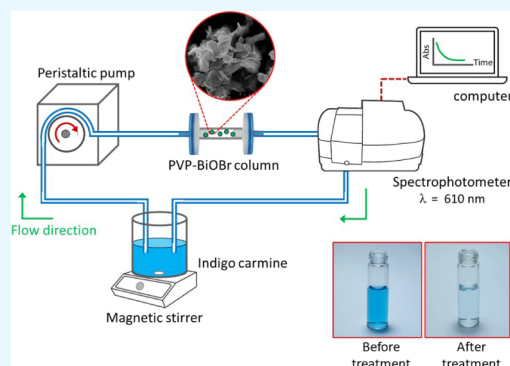
1. INTRODUCTION

Blue pigments are difficult to obtain from natural sources. Therefore, synthetic dyes such as indigo carmine (IC) are widely used, especially in food, textile, medical, and cosmetic manufacturing. Although the IC dye is commonly used in many industries, adverse effects on the environment and human health raise some concerns. Contamination of surface water by dyestuff increases turbidity and diminishes photosynthesis of aquatic plants.[1] These dyes can accumulate in aquatic animals, consequently entering the food chain. IC may cause skin irritation, vomiting, and diarrhea in humans.[2] According to the US and European Union regulations, the acceptable daily intake (ADI) of indigo carmine is limited to 2.5 and 5 mg kg^{-1} of body weight, respectively.[3] Therefore, it is necessary to remove color matter from industrial effluents before their discharge for environmental protection and human health.

Several methods have been proposed for the treatment of dye effluents. They include membrane filtration, bacterial decomposition, and photocatalysis as well as adsorption. The strengths and weaknesses of the various methods have been recently reviewed.[4] From our perspective, adsorption is an attractive method for wastewater treatment due to its simplicity and low investment. Adsorption is a physical or chemical process where the target contaminant is attached to the surfaces of an adsorbent material. Several alternative adsorbent materials have been presented for IC dye removal, for example, *Moringa oleifera* biomass,[5] magnesium ferrite nanoparticles,[6] ionic/nonionic polystyrene,[7] and COOH functionalized carbon nanotubes,[8] among others. Even though these adsorbents show great potential for dye removal, some limitations remain. Currently, most adsorbents are used under batch conditions with manual procedures.[6−8] After the adsorbents are exposed to water during treatment, it can be difficult to collect the resulting suspension. Therefore, separation and regeneration of adsorbent suspensions from treated water are some of the most challenging issues.[9] A promising flow-based method has been proposed for this challenge.[10−12]

In the past few years, many efforts have focused on bismuth oxybromide (BiOBr) composites, which have been shown to be very effective in adsorption and photodegradation. In previous studies, BiOBr composites demonstrated high
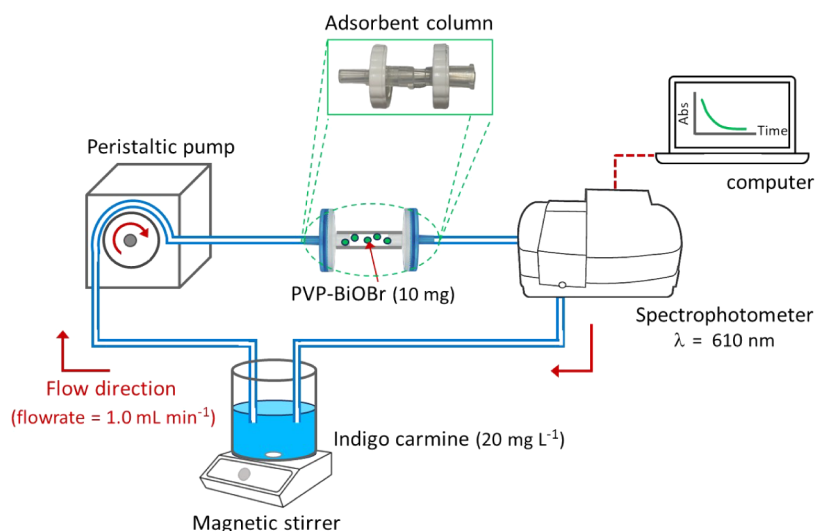
Figure 1. A flow-circulation manifold for continuous removal of indigo carmine using PVP-BiOBr as an absorbent.
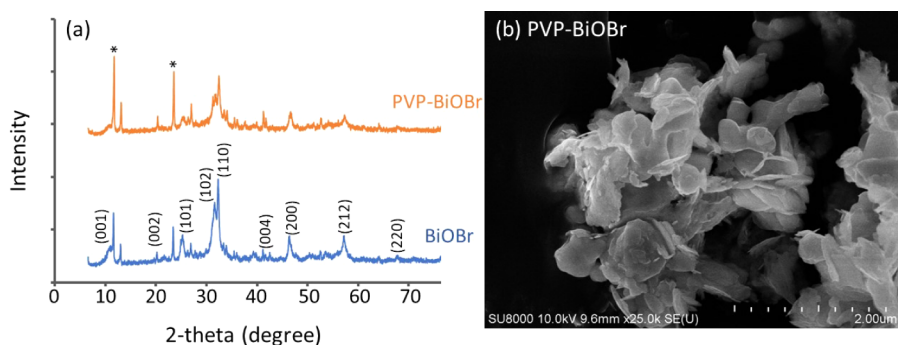
Figure 2. (a) XRD patterns of PVP-BiOBr compared to bare BiOBr. (b) SEM image of PVP-BiOBr.

performance in eliminating cylindrospermopsin and methylene blue.[13,14] Polyvinylpyrrolidone (PVP) is a hydrophilic polymer that is often employed as a stabilizing agent to regulate the morphologies, shapes, and sizes of particles.[15] Recently, Li et al. reported the use of PVP to improve the adsorption and photocatalytic capabilities of BiOBr.[16] To the best of our knowledge, there has been no report of the utilization of PVP modified BiOBr (PVP-BiOBr) for IC dye removal in a flow-based system. In the current work, PVP-BiOBr was synthesized using a facile one-step precipitation method and then used as an adsorbent for dye treatment. The morphology, surface area, and functional groups of the synthesized PVP-BiOBr were characterized. The adsorption isotherm and kinetic models were examined under batch condition. Then, a flow-circulation system was developed, and the removal efficiency of the dye by the system was explored. The advantages of a flow setup are that it is rapid and automated. PVP-BiOBr adsorbents are fixed in a column and do not contaminate water after the treatment.

2. EXPERIMENTAL SECTION

2.1. Chemicals and Apparatus. All chemicals were of analytical grade. Bismuth(III) nitrate pentahydrate and polyvinylpyrrolidone (MW 40 000) were purchased from Sigma-Aldrich, USA. Potassium bromide was received from Ajax Finechem, Australia. Absolute ethanol was obtained from Merck, Germany. Indigo carmine was purchased from HiMedia Laboratories, India. Deionized water (≥18.2 MΩ cm) was used throughout the experiments.

2.2. Synthesis of PVP-BiOBr. PVP-BiOBr was synthesized via a one-step precipitation method according to a previous report.[17] Briefly, 1.02 g of $Bi(NO_3)_3 \cdot 5H_2O$ was weighed and dissolved in 60 mL of ethanol with vigorous stirring for 60 min. A 0.05 g aliquot of PVP was incorporated into the bismuth nitrate solution and further stirred for 60 min. Then, 0.08 g of KBr was added to the solution, and the mixture was continuously stirred for an additional 12 h. After that, the mixture was centrifuged at 12 000 rpm for 10 min. A precipitate was collected and washed with DI water and ethanol at least 6 times. Finally, the product was dried at 60 °C for 6 h. For comparison, bare BiOBr was synthesized using a similar procedure but with no PVP addition.

2.3. Characterization. Synthesized PVP-BiOBr was characterized by using several techniques. The BiOBr crystal structure and purity were identified by using X-ray diffraction (XRD) (Smartlab Rigaku). Its morphology was observed under scanning electron microscopy (SEM) (SU8000 Hitachi). Specific surface area was analyzed with an N_2 adsorption−desorption isotherm employing the Brunauer−Emmett−Teller (BET) methodology. The pore size was calculated using a desorption isotherm in a Barret−Joyner−Halenda (BJH) approach (Micromeritics 3Flex). FTIR spectra were recorded using an FTIR spectrometer (Nicolet 6700 Thermo Scientific) at wavenumbers between 500 and 4000 cm^{-1}.

2.4. Flow-Circulation System. The flow system consisted of a peristaltic pump (ISM827B Ismatec), 1.0 mm ID PTFE

tubing, and a quartz flow-through cell (10 mm path length, Hellma Analytics). The adsorbent column was fabricated in our laboratory. It comprised two syringe filters (with a 0.45 μm nylon membrane) attached end-to-end. UV−vis absorption of indigo carmine was spectrophotometrically monitored (U2900 Hitachi) at a 610 nm wavelength. The flow manifold is depicted in Figure 1.

3. RESULTS AND DISCUSSION

3.1. PVP-BiOBr Characterization. XRD patterns of BiOBr and PVP-BiOBr are presented in Figure 2a. The main diffraction peaks of bare BiOBr were observed at $2\theta = 10.6°$, $21.7°$, $25.3°$, $31.6°$, $32.3°$, $42.5°$, $46.4°$, $57.2°$, and $67.6°$, which were indexed to the (001), (002), (101), (102), (110), (004), (200), (212), and (220) planes, corresponding to the tetragonal BiOBr standard (JCPDS no. 09−0393).[17] These characteristic peaks were also found in PVP-BiOBr, confirming the presence of the BiOBr crystal structure in the polymeric matrix. Peak intensities were weaker and broader in PVP-BiOBr compared to bare BiOBr. The crystallite size (D) of PVP-BiOBr was evaluated from the full width at half-maximum (fwhm) of the most intense peak ($2\theta = 32.4°$) using the Debye−Scherrer equation.[18] The average crystallite size was 19.7 nm. These XRD patterns show some impurity peaks (marked with asterisks) arising from the starting precursor $Bi(NO_3)_3·5H_2O$.

The morphology of PVP-BiOBr was observed under SEM, and the results are shown in Figure 2b. The sample exhibits an assembly of several thin-petal nanosheets, similar to an earlier report.[17] The mean particle size was ∼2.0 μm. The EDX spectrum of the PVP-BiOBr is depicted in Figure S1 indicating the presence of bismuth, oxygen, and bromine elements in the sample.

Figure 3 illustrates that the PVP-BiOBr adsorbent exhibits the characteristic type III N_2 adsorption−desorption under the
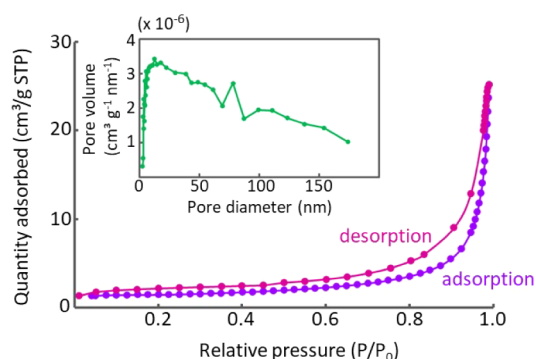
Figure 3. Nitrogen adsorption−desorption isotherm and BJH pore size distribution plot (inset) of the as-prepared PVP-BiOBr.

IUPAC classification.[19] This type III characteristic indicates a morphology consisting of both micro- and mesoporous structures. The inset of Figure 3 shows that the peak pore-size distribution of the prepared adsorbent was ∼12.7 nm. The BET specific surface area of the PVP-BiOBr adsorbent was 5.14 m² g⁻¹, which is significantly higher than that of bare BiOBr (1.107 m² g⁻¹).

In the presence of PVP during precipitation synthesis, PVP could coordinate on the surface of the BiOBr crystallographic planes and control the growth of the crystal facets. This results in a petal-like morphology and an increased specific surface

area.[15] Owing to its porous structure with large surface area, PVP-BiOBr can thus provide abundant active sites to interact with organic pollutants, which extensively promotes adsorption. For comparison, an SEM image of bare BiOBr is shown in Figure S2. Without PVP, the BiOBr exhibits a flake-like morphology. The potential of the prepared PVP-BiOBr for adsorptive removal of IC dye was further studied.

3.2. Investigation of IC Dye Removal Mechanism by PVP-BiOBr (Batch Experiment). It is established that PVP-BiOBr exhibits both photocatalytic and adsorptive properties, and thus is widely used to remediate organic contamination.[13,14,16] In this study, the primary mechanism of PVP-BiOBr to eliminate the IC dye is elucidated. Batch experiments were performed with and without light radiation. A 10 mg portion of PVP-BiOBr was added to a 50 mL solution of IC dye (20 mg L⁻¹). The solution was stirred for 60 min. While stirring, 3 mL of the dye solution was sampled at preset time intervals. This sample was centrifuged for 3 min, and then the supernatant was spectrophotometrically measured at a 610 nm wavelength. The concentration of IC dye remaining in the solution was assessed and the percentage of dye removal (%R) was:

$$\%R = \left(\frac{C_0 - C_t}{C_0} \right) \times 100 \tag{1}$$

where C_0 and C_t are the initial concentration and concentration at time t of IC dye in solution (mg L⁻¹), respectively.

Two beakers of the dye solution were tested. The first beaker was stirred and irradiated by fluorescent lamps (24 W × 2 lamps), while the second beaker was stirred under dark conditions in a black box. The dye removal under these two conditions is depicted in Figure 4a. The percentage of dye removal with and without light illumination both showed a dye elimination of up to ∼85% after 15 min. This implies that light negligibly impacted the removal process. PVP-BiOBr provides adsorptive performance toward IC dyes rather than photo-catalytic activity. The photocatalysis level parameter (ξ) was also evaluated to further understand the effect of adsorption/photocatalysis on dye elimination. The parameter ξ was defined as the ratio of the total removal amount in adsorption−photocatalysis to the adsorption removal amount in the dark.[20] As observed in Figure S3, the ξ parameter exhibited a downward tendency after 5 min. It is explained that the adsorbed IC on the PVP-BiOBr impeded photocatalysis by shielding the material surfaces from light.[21] Therefore, in this work, PVP-BiOBr was proposed as an efficient adsorbent for IC dye removal.

Additionally, the adsorptive performance of BiOBr and PVP-BiOBr for IC dye molecules was compared. These two absorbents were dispensed into IC solutions for 15 min, and the remaining dye concentrations were subsequently analyzed. Only 66.2% of IC dye was removed by BiOBr, while 85.4% was eliminated using PVP-BiOBr. Owing to its larger surface area, PVP-BiOBr offers a greater adsorption of dye molecules. FTIR analysis was used to clarify the interaction of IC dye adsorbed onto the PVP-BiOBr adsorbent. The FTIR spectra of IC, PVP-BiOBr, and PVP-BiOBr@IC are shown in Figure 4b. PVP-BiOBr@IC displays characteristic bands of both pure IC and PVP-BiOBr that are slightly shifted toward lower wave-numbers. For example, the wavenumber of the carbonyl group in the PVP-BiOBr was shifted from 1617.73 cm⁻¹
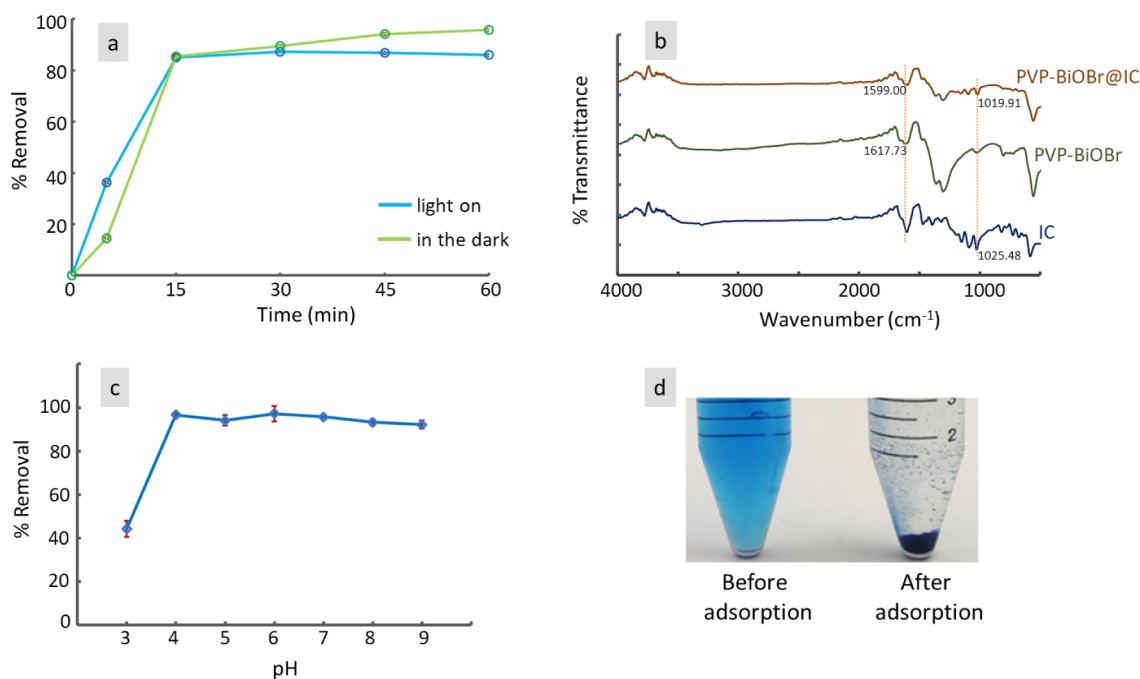
Figure 4. (a) IC removal using PVP-BiOBr under light irradiation and under dark conditions, (b) FITR spectra of IC, PVP-BiOBr and PVP-BiOBr@IC, (c) effect of pH on %removal of IC, and (d) images of an indigo carmine solution before and after adsorption by PVP-BiOBr.
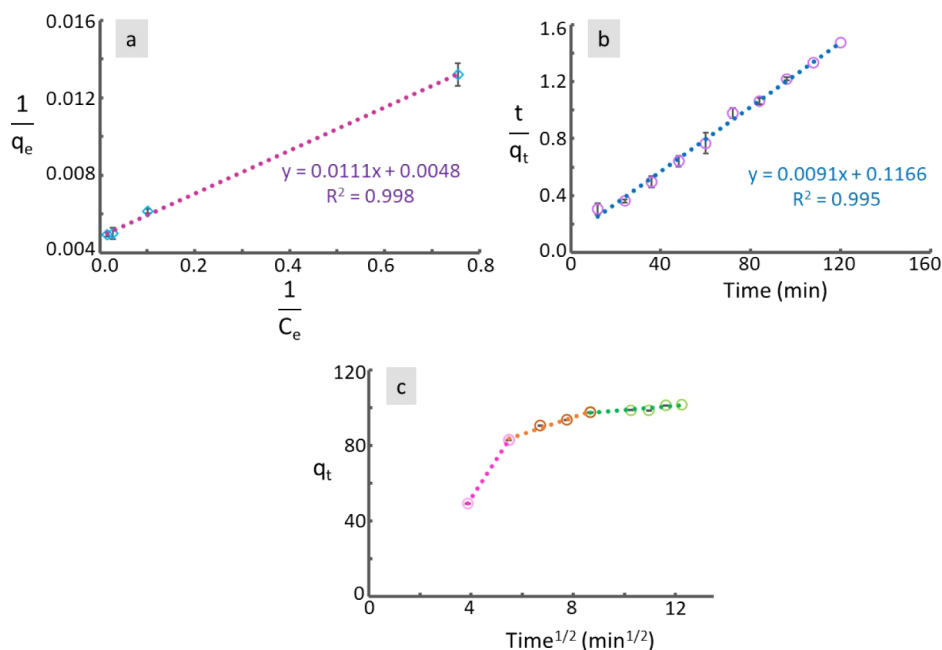
Figure 5. Plots of (a) Langmuir isotherm, (b) pseudo-second-order kinetics, and (c) intraparticle diffusion models for IC removal by PVP-BiOBr.

(before adsorption) to 1599.00 cm^{-1} (after adsorption). Concurrently, the sulfonyl bands of PVP-BiOBr@IC were located at 1019.91 cm^{-1}, which is a lower wavenumber than that of pure IC (1025.48 cm^{-1}). These results infer bond formation between IC molecules and adsorbent surfaces.[22]

3.3. Effect of PVP Composition. The adsorptive performance of PVP-BiOBr may be dependent on the PVP component. Therefore, different amounts of PVP (i.e., 0.02, 0.05, and 0.10 g) were used in the synthesis of the PVP-BiOBr adsorbents. Subsequently, each adsorbent was tested for its dye removal capability. The adsorbent made with 0.05 g PVP manifested the greatest IC removal efficiency, 97.0% after 45

min, while 80.5% and 91.7% of IC were reduced using the adsorbents with 0.02 and 0.10 g PVP, respectively. In this work, 0.05 g of PVP was thus selected for the adsorbent preparation.

3.4. Effect of pH. The effect of pH on IC dye removal was examined by adjusting the initial pH of IC solutions from 3 to 9 using 0.1 M HCl or NaOH solutions as appropriate. As shown in Figure 4c, at very low pH (pH = 3), abundant protons may retard the adsorption process, and the removal percentage was low. At higher pH, dye removal sharply increased and maintained its efficiency in the pH range from 4 to 9. This demonstrated that the PVP-BiOBr adsorbent can be
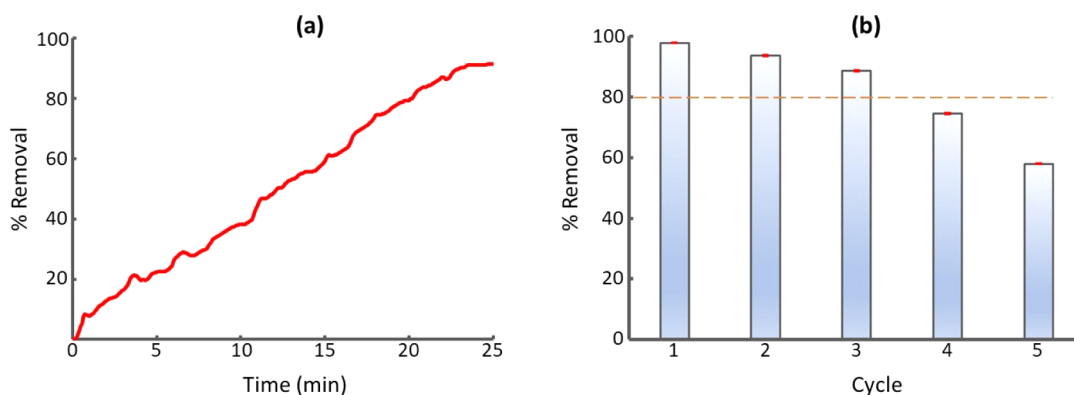
Figure 6. (a) The %removal of IC dye as a function of time in the flow system and (b) reusability of the PVP-BiOBr adsorbent for 5 consecutive cycles.

effectively used over a wide pH range. Hence, pretreatment pH adjustments are not required for water samples with pH values ranging from 4 to 9. Images of indigo carmine solutions before and after adsorption by PVP-BiOBr are shown in Figure 4d.

3.5. Adsorption Isotherm. Isotherms, such as the Langmuir and Freundlich models, are commonly used for equilibrium adsorption in a solution of adsorbed molecules and adsorbent surfaces. In this work, the experimental data were better fitted by the Langmuir model, represented in eq 2, with a linear correlation $(R^2) = 0.998$ (Figure 5a).

$$\frac{1}{q_e} = \left(\frac{1}{q_{max}K_L}\right)\left(\frac{1}{C_e}\right) + \left(\frac{1}{q_{max}}\right) \qquad (2)$$

where q_e is the adsorption capacity of IC at equilibrium (mg g^{-1}), C_e is the concentration of IC in the aqueous phase at equilibrium (mg L^{-1}), q_{max} is the maximum adsorption capacity of IC per unit weight of the adsorbent (mg IC/g of PVP-BiOBr), and K_L is the Langmuir constant (L mg^{-1}). For the results shown in Figure 5a and using eq 2, the q_{max} and K_L values were 208.3 mg g^{-1} and 0.432 L mg^{-1}, respectively. The Langmuir model leads to an assumption that the IC molecules are adsorbed on the PVP-BiOBr surface as a monolayer, and maximum adsorption occurs when the surface is entirely covered.

3.6. Kinetics Study and Intraparticle Diffusion. Adsorption kinetics and intraparticle diffusion were examined to determine the adsorption rate and mechanism. In this study, the experimental data were applied to pseudo-first- and pseudo-second-order kinetics models. The adsorption kinetics were in accordance with a pseudo-second-order model (eq 3). The measured R^2 value of the plot between t/q_t and t was 0.995 (Figure 5b).

$$\frac{t}{q_t} = \frac{1}{k_2 q_e^2} + \left(\frac{1}{q_e}\right)t \qquad (3)$$

where k_2 is the equilibrium rate constant of the pseudo-second-order model (g mg^{-1} min^{-1}) and q_t denotes the amount of IC adsorbed at time t. The slope and intercept in Figure 5b were used to find the rate constant k_2, 7.10×10^{-4} g mg^{-1} min^{-1}. A pseudo-second-order kinetic model suggests that the rate-limiting step is surface adsorption. The adsorption rate is dependent on adsorption capacity and not on dye concentration.

The adsorption mechanism generally involves three mass transfer steps, i.e., (i) external diffusion, (ii) internal diffusion, and (iii) adsorption onto active sites. The adsorption mechanism was determined by employing the intraparticle diffusion equation given by eq 4.

$$q_t = k_i t^{1/2} \qquad (4)$$

where k_i is the intraparticle diffusion rate (mg g^{-1} min$^{-1/2}$). In the current work, a plot of q_t versus $t^{1/2}$ revealed multi-linearities (Figure 5c). This implies that multiple steps occurred that limited the overall adsorption rate. The first sharp range describes fast diffusion of the IC dye in the solution boundary to the external surface of the PVP-BiOBr adsorbent. The second range was attributed to gradual adsorption into the adsorbent micropores, while the third plateau indicated that an equilibrium was reached in which the adsorption became slow and stable. The plots did not pass through the origin, which indicates that the intraparticle diffusion was not the only rate-controlling step, but boundary diffusion controlled adsorption to some degree.[23]

3.7. Flow-Circulation for IC Removal. The flow-circulation system in Figure 1 was employed for indigo carmine dye removal. A 10 mL volume of an IC solution (20 mg L^{-1}) was pipetted into a container. The solution pH was adjusted to pH ~7. The solution was transferred into the flow-circulation system using a peristaltic pump with a flow rate of 1.0 mL min^{-1}. A portion of 10 mg of PVP-BiOBr was placed in the adsorbent column. A nylon membrane retained the adsorbent inside the column. When an IC solution passed through the column, some of it was removed by the PVP-BiOBr adsorbent. The residues were measured inline by using a spectrophotometer positioned after the column. They were recirculated in the flow system, and %removal was continuously monitored as a function of time (Figure 6a).

The dye was gradually eliminated and reached ≥90% removal after 25 min of flow. With this flow-circulation system, the adsorbents are retained in a column and do not contaminate the water sample after treatment. The system is operated inline, automated, and convenient to use. It can be further developed for commercial-scale water treatment applications. Reusability of the adsorbent column was also investigated. After the first treatment, the column was regenerated by being flushed with water before use in a second run. The PVP-BiOBr adsorbents retained a removal efficiency of over 80% even after the third run, suggesting good stability and reusability (Figure 6b). The adsorption capacities

Table 1. Comparison of Adsorption Capacities of Various Adsorbents for IC Dye Removal

adsorbent	operation mode	maximum adsorption capacity (mg/g)	suitable solution pH	regeneration (cycles)	ref.
Moringa oleifera seeds	batch/fixed-bed column	60.24	4	4	5
magnesium ferrite nanoparticles	batch	46	4−9	4	6
ionic/nonionic polystyrene	batch	-	≥10	-	7
COOH functionalized carbon nanotubes	batch	136	6	8	8
Bismuth oxide doped MgO	batch	126	7	3	24
Acacia nilotica sawdust activated carbon	fixed-bed column	24.67	-	-	
PVP-BiOBr	flow-circulation	208.3	4−9	3	this work

of various adsorbents toward IC dye are compared as presented in Table 1. Furthermore, the effectiveness of PVP-BiOBr to remove IC dye was compared with that of commercial activated carbon (Vikings, Thailand). The % removal of IC dye by PVP-BiOBr was higher than that of activated carbon (Figure S4). This absorbent has the potential for removing IC dye from contaminated water samples.

4. CONCLUSIONS

The PVP-BiOBr adsorbent was successfully prepared through a facile precipitation method. The PVP polymer plays a crucial role in controlling the morphology, size, surface area, and adsorption efficiency of the adsorbent. With its greater surface area, PVP-BiOBr afforded a higher adsorptive performance for IC dye removal than bare BiOBr. The characteristics of prepared PVP-BiOBr are summarized in Table S1. The adsorption isotherm fitted the Langmuir model, and the maximum adsorption capacity was 208.3 mg g^{-1}. The adsorption kinetics were in good agreement with a pseudo-second-order model. A suitable pH for IC adsorption ranged from 4 to 9. A flow-circulation system using a PVP-BiOBr column was applied for the water treatment. Its efficiency reached ≥90% removal of the IC dye. The adsorbent column was used for three cycles. The adsorption efficiency of PVP-BiOBr was higher than that for commercially available activated carbon. The advantages of the flow system are that (i) it is an inline and continuous process with (ii) easy separation of the adsorbent from treated water. It is a promising method for wastewater treatment.

ASSOCIATED CONTENT

Supporting Information

The Supporting Information is available free of charge at https://pubs.acs.org/doi/10.1021/acsomega.4c02973.

> SEM image, EDX spectrum, graph of the photocatalysis level parameter, %removal of IC dye using different adsorbents, and summary of characteristics of PVP-BiOBr (PDF)

AUTHOR INFORMATION

Corresponding Author

Saowapak Teerasong − *Flow Innovation-Research for Science and Technology Laboratories (FIRST Laboratories), Bangkok 10520, Thailand; Department of Chemistry and Applied Analytical Chemistry Research Unit, School of Science, King Mongkut's Institute of Technology Ladkrabang, Bangkok 10520, Thailand;* orcid.org/0009-0008-7744-5661; Email: saowapak.te@kmitl.ac.th

Authors

Thanakrit Saenghirun − *Department of Chemistry and Applied Analytical Chemistry Research Unit, School of Science, King Mongkut's Institute of Technology Ladkrabang, Bangkok 10520, Thailand*

Thanawat Sunthornchainukul − *Department of Chemistry and Applied Analytical Chemistry Research Unit, School of Science, King Mongkut's Institute of Technology Ladkrabang, Bangkok 10520, Thailand*

Supinya Thammaso − *Department of Chemistry and Applied Analytical Chemistry Research Unit, School of Science, King Mongkut's Institute of Technology Ladkrabang, Bangkok 10520, Thailand*

Apiwat Chompoosor − *Department of Chemistry and Center of Excellence for Innovation in Chemistry, Faculty of Science, Ramkhamhaeng University, Bangkok 10240, Thailand;* orcid.org/0000-0003-3746-0468

Suwat Nanan − *Materials Chemistry Research Center, Department of Chemistry and Center of Excellence for Innovation in Chemistry, Faculty of Science, Khon Kaen University, Khon Kaen 40002, Thailand;* orcid.org/0000-0002-8737-689X

Complete contact information is available at:
https://pubs.acs.org/10.1021/acsomega.4c02973

Author Contributions

S.T. contributed to conceptualization, formal analysis, validation, funding acquisition, writing − original draft, and supervision. T. Sunthornchainukul, T. Saenghirun, and S.T. contributed to investigation and methodology. A.C. contributed to validation and writing − review and editing. S.N. contributed to writing − review and editing. All authors have approved the manuscript for publication.

Notes

The authors declare no competing financial interest.

ACKNOWLEDGMENTS

REFERENCES

(1) Rendon-Castrillón, L.; Ramírez-Carmona, M.; Ocampo-López, C.; González-López, F.; Cuartas-Uribe, B.; Mendoza-Roca, J. A. Treatment of water from the textile industry contaminated with indigo dye: A hybrid approach combining bioremediation and

nanofiltration for sustainable reuse. *Case Stud. Chem. Environ. Eng.* **2023**, *8*, 100498.

(2) Pereira, P. C. G.; Reimão, R. V.; Pavesi, T.; Saggioro, E. M.; Moreira, J. C.; Correia, F. V. Lethal and sub-lethal evaluation of Indigo Carmine dye and byproducts after TiO_2 photocatalysis in the immune system of *Eisenia andrei* earthworms. *Ecotoxicol. Environ. Saf.* **2017**, *143*, 275−282.

(3) Lehto, S.; Buchweitz, M.; Klimm, A.; Straßburger, R.; Bechtold, C.; Ulberth, F. Comparison of food colour regulations in the EU and the US: a review of current provisions. *Food Addit. Contam., Part A* **2017**, *34*, 335−355.

(4) Chowdhury, M. F.; Khandaker, S.; Sarker, F.; Islam, A.; Rahman, M. T.; Awual, M. R. Current treatment technologies and mechanisms for removal of indigo carmine dyes from wastewater: A review. *J. Mol. Liq.* **2020**, *318*, 114061.

(5) El-Kammah, M.; Elkhatib, E.; Gouveia, S.; Cameselle, C.; Aboukila, E. Enhanced removal of indigo carmine dye from textile effluent using green cost-efficient nanomaterial: Adsorption, kinetics, thermodynamics and mechanisms. *Sustain Chem. Pharm.* **2022**, *29*, 100753.

(6) Adel, M.; Ahmed, M. A.; Mohamed, A. A. Effective removal of indigo carmine dye from wastewaters by adsorption onto mesoporous magnesium ferrite nanoparticles. *Environ. Nanotechnol. Monit. Manag.* **2021**, *16*, 100550.

(7) Pan, J.; Zhou, L.; Chen, H.; Liu, X.; Hong, C.; Chen, D.; Pan, B. Mechanistically understanding adsorption of methyl orange, indigo carmine, and methylene blue onto ionic/nonionic polystyrene adsorbents. *J. Hazard. Mater.* **2021**, *418*, 126300.

(8) Dastgerdi, Z. H.; Meshkat, S. S.; Esrafili, M. D. Enhanced adsorptive removal of Indigo carmine dye performance by functionalized carbon nanotubes based adsorbents from aqueous solution: equilibrium, kinetic, and DFT study. *J. Nanostruct. Chem.* **2019**, *9*, 323−334.

(9) Du, Z.; Liu, F.; Ding, G.; Dan, Y.; Jiang, L. Effective degradation of tetracycline via polyvinyl alcohol /Bi_2WO_6 hybrid hydrogel with easy separation. *Mater. Chem. Phys.* **2021**, *262*, 124239.

(10) Gupta, T.; Ansari, K.; Lataye, D.; Kadu, M.; Khan, M. A.; Mubarak, N. M.; Garg, R.; Karri, R. R. Adsorption of indigo carmine dye by Acacia nilotica sawdust activated carbon in fixed bed column. *Sci. Rep.* **2022**, *12*, 15522.

(11) Vairavel, P.; Rampal, N. Continuous fixed-bed column study for removal of Congo red dye from aqueous solutions using Nelumbo nucifera leaf adsorbent. *Int. J. Environ. Anal. Chem.* **2023**, *103*, 5025−5044.

(12) Selambakkannu, S.; Othman, N. A. F.; Bakar, K. A.; Karim, Z. A. Adsorption studies of packed bed column for the removal of dyes using amine functionalized radiation induced grafted fiber. *SN Appl. Sci.* **2019**, *1*, 175.

(13) Shi, Y.; Li, J.; Huang, D.; Wang, X.; Huang, Y.; Chen, C.; Li, R. Specific adsorption and efficient degradation of cylindrospermopsin on oxygen-vacancy sites of BiOBr. *ACS Catal.* **2023**, *13*, 445−458.

(14) Wang, D.; Shen, H.; Guo, L.; Wang, C.; Fu, F. Porous BiOBr/Bi_2MoO_6 heterostructures for highly selective adsorption of methylene blue. *ACS Omega* **2016**, *1*, 566−577.

(15) Bárdos, E.; Márta, V.; Baia, L.; Todea, M.; Kovács, G.; Baán, K.; Garg, S.; Pap, Z.; Hernadi, K. Hydrothermal crystallization of bismuth oxybromide (BiOBr) in the presence of different shape controlling agents. *Appl. Surf. Sci.* **2020**, *518*, 146184.

(16) Li, Y.; Wang, Z.; Huang, B.; Dai, Y.; Zhang, X.; Qin, X. Synthesis of BiOBr-PVP hybrids with enhanced adsorption-photocatalytic properties. *Appl. Surf. Sci.* **2015**, *347*, 258−264.

(17) Zhang, B.; Zhang, M.; Zhang, L.; Bingham, P. A.; Li, W.; Kubuki, S. PVP surfactant-modified flower-like BiOBr with tunable bandgap structure for efficient photocatalytic decontamination of pollutants. *Appl. Surf. Sci.* **2020**, *530*, 147233.

(18) Senasu, T.; Chankhanittha, T.; Hemavibool, K.; Nanan, S. Solvothermal synthesis of BiOBr photocatalyst with an assistant of PVP for visible-light-driven photocatalytic degradation of fluoroquinolone antibiotics. *Catal. Today* **2022**, *384−386*, 209−227.

(19) Thommes, M.; Kaneko, K.; Neimark, A. V.; Olivier, J. P.; Rodriguez-Reinoso, F.; Rouquerol, J.; Sing, K. S. W. Physisorption of gases, with special reference to the evaluation of surface area and pore size distribution (IUPAC technical report). *Pure Appl. Chem.* **2015**, *87*, 1051−1069.

(20) Liu, M.; Zou, D.; Ma, T.; Liu, Z.; Li, Y. Simultaneously efficient adsorption and accelerated photocatalytic degradation of chlortetracycline hydrochloride over novel Fe-based MOGs under visible light irradiation cooperated by hydrogen peroxide. *Inorg. Chem. Front.* **2019**, *6*, 1388−1397.

(21) Sun, Y.; Gao, Y.; Li, Y.; Zou, D. Novel bifunctional in-based metal−organic gel/bacterial cellulose composite gels for effective tetracycline antibiotics removal: Synergistic behavior and mechanism insight of adsorption-photocatalysis. *Chem. Eng. J.* **2023**, *475*, 146107.

(22) Du, R.; Cao, H.; Wang, G.; Dou, K.; Tsidaeva, N.; Wang, W. PVP modified rGO/$CoFe_2O_4$ magnetic adsorbents with a unique sandwich structure and superior adsorption performance for anionic and cationic dyes. *Sep. Purif. Technol.* **2022**, *286*, 120484.

(23) Ojedokun1, A. T.; Bello, O. S. Kinetic modeling of liquid-phase adsorption of Congo red dye using guava leaf-based activated carbon. *Appl. Water Sci.* **2017**, *7*, 1965−1977.

(24) Adam, F. A.; Ghoniem, M. G.; Diawara, M.; Rahali, S.; Abdulkhair, B. Y.; Elamin, M. R.; Aissa, M. A. B.; Seydou, M. Enhanced adsorptive removal of indigo carmine dye by bismuth oxide doped MgO based adsorbents from aqueous solution: equilibrium, kinetic and computational studies. *RSC Adv.* **2022**, *12*, 24786−24803.